

Crystal Structure and Transport Properties in the $\text{Ba}_8\text{Zn}_x\text{Ge}_{46-x-y}[\]_y$ Clathrates

E. Alleno, G. Maillet, O. Rouleau, E. Leroy, C. Godart

ICMPE-CMTR, CNRS-UMR7182, 2-8 rue H. Dunant, 94320 THIAIS, FRANCE

eric.alleno@icmpe.cnrs.fr

Abstract

In the $\text{Ba}_8\text{Zn}_x\text{Ge}_{46-x-y}[\]_y$ ($4 < x < 8$, $[\] = \text{vacancy}$) series, the clathrate type I structure is only a good approximant: a $4ax4ax4a$ superstructure is indicated by our X-ray powder measurements. Electron probe micro-analysis performed on polycrystalline samples with $2 \leq x \leq 8$ shows that the fraction of vacancies varies like $y = 3.3-x/2$ for $x \leq 6$ and that $y = 0$ for $x > 6$. It also confirms that Zn first substitutes Ge and $[\]$ on the 6c site of the approximant type I structure. Resistivity versus temperature (5K-300K) data ($x > 6$) are in line with a degenerate semi-conducting behaviour and evolves monotonously with x and the electron density (Hall effect). The room temperature Seebeck coefficient increases with x and reaches $-67.1 \mu\text{V/K}$ in $\text{Ba}_8\text{Zn}_8\text{Ge}_{30}$ which also shows the largest power factor in our series. Assuming a thermal conductivity ($\lambda = 1.5 \text{ W}\cdot\text{m}^{-1}\text{K}^{-1}$) similar to $\text{Ba}_8\text{Ga}_{16}\text{Ge}_{30}$, $ZT = 0.07$ at 300K in $\text{Ba}_8\text{Zn}_8\text{Ge}_{38}$.

Introduction

Type I inorganic clathrates $\text{A}_8\text{M}_x\text{X}_{46-x}[\]_y$ ($[\] = \text{vacancy}$) are compounds built by group IV elements (X), substituted either by group VIII, IB, IIB or IIIA elements (M), which form large 20- and 24-atom cages filled by electropositive group IIA elements (A). The $\text{M} = \text{Ga}$ and $\text{X} = \text{Ge}$ compounds attracted great interest because of their potential for thermoelectricity generation: the $\text{A}_8\text{Ga}_{16}\text{Ge}_{30}$ ($\text{A} = \text{Sr}, \text{Ba}, \text{Eu}$) clathrates display ZT values larger than 1 at 800-900K [1-4]. They belong to the ‘‘Phonon Glass and Electron Crystal’’ class of materials since the localized vibrations of the electropositive group II element in the 20- and 24-atom cages are thought to resonantly scatter the heat-carrying phonons and strongly reduce the lattice thermal conductivity to values as low as $1 \text{ W}\cdot\text{m}^{-1}\cdot\text{K}^{-1}$ [1]. Despite their ‘‘glass-like’’ lattice thermal conductivity, the $\text{A}_8\text{Ga}_{16}\text{Ge}_{30}$ compounds exhibit Seebeck (α) coefficients and electrical resistivity (ρ) typical of crystalline degenerate semiconductors which can be ascribed to the $[\text{Ga}_{16}\text{Ge}_{30}]$ subnetwork: in single crystalline $\text{Ba}_8\text{Ga}_{16}\text{Ge}_{30}$, $\rho = 0.7 \text{ m}\Omega\cdot\text{cm}$ and $\alpha = -50 \mu\text{V}\cdot\text{K}^{-1}$ at 300K [2]. Band structure calculations in $\text{A}_8\text{Ga}_x\text{Ge}_{46-x}[\]_y$ ($\text{A} = \text{Sr}, \text{Ba}, \text{Eu}$) confirmed that these compounds fulfil the Zintl rules: the eight A^{2+} atoms fully donate their 16 electrons to the gallium and to the vacancies which behave as acceptors [5, 6].

The $\text{Ba}_8\text{Zn}_x\text{Ge}_{46-x-y}[\]_y$ compounds were first reported by Kuhl et al [7] who concluded that the $4 \leq x \leq 8$ compounds crystallizes within the clathrate type I structure. The transport properties in $\text{Ba}_8\text{Zn}_x\text{Ge}_{46-x-y}[\]_y$ are unknown except that Kuhl et al. speculated the relation $y = 4-x/2$ between the zinc and vacancies concentrations which implies complete charge compensation and semiconducting properties all along the series. This speculation seemed promising for the

thermoelectric properties of the Zn-based clathrates since the highest power factors (α^2/ρ) were found in Ga-based type I clathrates with formally complete charge compensation ($x(\text{Ga}) = 16$) [8]. We therefore decided to explore the unknown electronic transport properties of the $\text{Ba}_8\text{Zn}_x\text{Ge}_{46-x-y}[\]_y$ series as a function of the compositional parameters x and y .

Experimental

The $\text{Ba}_8\text{Zn}_x\text{Ge}_{46-x-y}[\]_y$ ($x = 2-4, 6-8, y = 0-3$) polycrystalline samples were obtained in a two steps synthesis. Ba (99%, with 3% mass-excess) and Ge (99.999%) were first arc-melted on a copper hearth under argon. This coarsely crushed button was introduced in a vitreous carbon crucible and the proper amount of Zn (99.9%) was added. This crucible was then introduced in a quartz tube which was sealed under partial Ar atmosphere and heated to 980°C for 12 hours and annealed for 4-6 days at 900°C. Two $x = 8$ samples labelled A and B were melted.

X-ray powder diffraction intensities ($\text{Cu K}\alpha$ radiation) were recorded in the $[10^\circ-110^\circ]$ 2θ range on a Brüker D8 diffractometer. The patterns were refined using the program FULLPROF [9] either implementing the Rietveld method or Le Bail’s method [10]. Electron Probe Micro-Analysis (EPMA) of the barium, zinc and germanium concentrations was performed with a CAMECA SX100 electron microprobe ($V = 15\text{kV}$, $I = 60\text{nA}$) using BaSO_4 , ZnSe and Ge as standards.

Seebeck coefficient measurements were made on $8 \times 1.5 \times 1.5\text{mm}^3$ bar-shaped samples at room temperature using a homemade apparatus with Chromel/Constantan thermocouples, as described in ref [11], with a constant thermal gradient $\Delta T = 1\text{K}$. Electrical resistivity and Hall effect measurements (0-5T) were performed on square shape samples ($\sim 4 \times 4 \times \sim 0.4 \text{ mm}^3$) between 5K and 300K using the Van der Paw method in a Quantum Design PPMS in ac mode ($\nu = 107 \text{ Hz}$).

Structural and chemical analysis

Initially, the diffraction patterns of our $\text{Ba}_8\text{Zn}_x\text{Ge}_{46-x-y}[\]_y$ samples were Rietveld-refined within the type I clathrate structure. An example of such a refinement is shown in Fig. 1a for $\text{Ba}_8\text{Zn}_8\text{Ge}_{38}$ (sample A) with a lattice parameter $a = 10.763 \text{ \AA}$ close to the value reported by Kuhl et al. [7]. The derived lattice parameters (a) for the whole series are gathered in Table I. Despite the good reliability factor ($R_p = 7.5\%$) obtained, it can be noticed that faint satellite lines belonging to the $\text{Ba}_8\text{Zn}_8\text{Ge}_{38}$ phase (marked with arrows) cannot be indexed within the clathrate type I structure. We also failed to index all the diffraction lines in $\text{Ba}_8\text{Zn}_8\text{Ge}_{38}$ within a distorted type I structure with a monoclinic unit

cell, or within a type I structure combined with an incommensurate structure modulation. As can be seen in Fig. 1b, a satisfactory indexation was obtained by using a cubic superstructure with $a' = 4a = 43.052 \text{ \AA}$ ($R_p = 4.3\%$, Le Bail's method). These superstructure lines can unambiguously be observed in all our samples except the $x = 2$ sample were the lines corresponding to large amount of a secondary phase ($\text{Ba}_6(\text{Zn/Ge})_{25}$, see below) overlaps with many of the superstructure lines. Nonetheless, for the sake of uniformity, the $x = 2$ pattern was treated similarly to the other patterns. Thus, this X-ray powder work indicate that for $x > 2$, the $\text{Ba}_8\text{Zn}_x\text{Ge}_{46-x-y}[\]_y$ compounds crystallize within a superstructure variant ($a' = 4a$) of the classical clathrate type I structure. To confirm and completely determine this superstructure, a single crystal work will be required. Despite the fact that the $\text{Ba}_8\text{Zn}_x\text{Ge}_{46-x-y}[\]_y$ do not crystallize within the clathrate type I structure, this last structure remains a good approximant since we found good Rietveld reliability factors and since it had previously been ascribed to these compounds in a single crystal X-ray work [7]. Therefore, in the rest of this text, we keep the labeling of the type I structure sites and the $8/x/46-x-y/y$ stoichiometry to describe these zinc-based clathrates. This choice is consistently confirmed by our EPMA elemental analysis.

The results of the chemical analysis of the phases occurring in the $\text{Ba}_8\text{Zn}_x\text{Ge}_{46-x-y}[\]_y$ samples are summarized in Table I. The elemental composition measurements confirmed that the $x = 4-8$ samples contain the $\text{Ba}_8\text{Zn}_x\text{Ge}_{46-x-y}[\]_y$ clathrate as the majority phase with the measured zinc concentration $[\text{Zn}]$ very close to its nominal value. Only few inclusions of BaZn_2Ge_2 in the $x = 8$ sample (B) and $\text{Ba}_6(\text{Zn/Ge})_{25}$ in the $x = 4$ sample could be detected as secondary phases. The $x = 6$ sample is single phase. The $x = 2$ sample displays a multiphase microstructure with $\text{Ba}_8\text{Zn}_{2.3}\text{Ge}_{41.5}$ and $\text{Ba}_6(\text{Zn/Ge})_{25}$ as the main phases (measured composition) and large inclusions of Ge at the grain boundaries. Despite this equilibrium situation between these three phases in the $x = 2$ sample, the measured composition $\text{Ba}_8\text{Zn}_{2.34}\text{Ge}_{41.54}$ shows that the phase " $\text{Ba}_8\text{Zn}_2\text{Ge}_{42}[\]_2$ " exists. This elemental analysis is consistent with the X-ray analysis which gave the same phase

identification and moreover yielded the mass percentage of each phase.

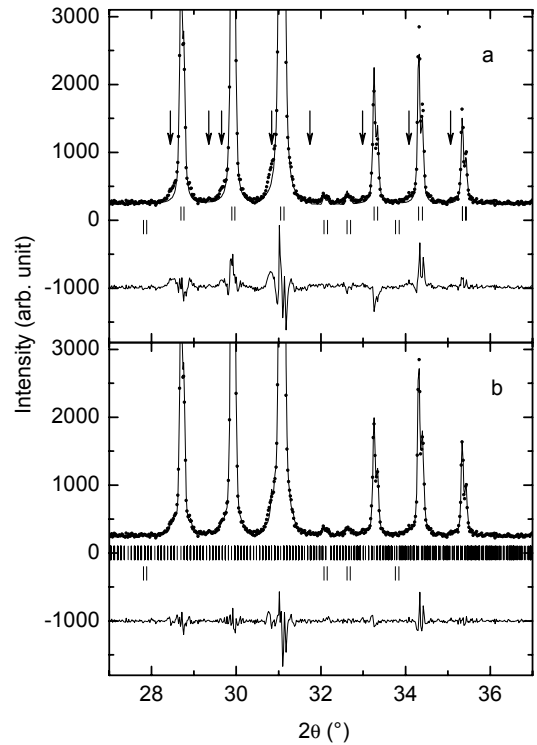


Figure 1. a- Experimental (circle) and calculated (line) diffraction pattern of the $\text{Ba}_8\text{Zn}_8\text{Ge}_{38}$ sample (A). The bottom sets of small vertical lines correspond to the Bragg positions of the two contributions to the pattern ($\text{Ba}_8\text{Zn}_8\text{Ge}_{38}$ type I clathrate and BaZn_2Ge_2). b- diffraction pattern of the $\text{Ba}_8\text{Zn}_8\text{Ge}_{38}$ sample (A) indexed by the cubic superstructure $a = 4a'$ of the type I clathrate structure.

Nominal composition	a (Å)	a' (Å)	Measured composition	Secondary phases
$\text{Ba}_8\text{Zn}_8\text{Ge}_{38}$ (A)	10.763	43.052	$\text{Ba}_{7.95(3)}\text{Zn}_{7.83(6)}\text{Ge}_{38.17(6)}$	3% BaZn_2Ge_2
$\text{Ba}_8\text{Zn}_8\text{Ge}_{38}$ (B)	10.762	43.048	$\text{Ba}_{7.93(3)}\text{Zn}_{7.53(3)}\text{Ge}_{38.47(4)}$	4% BaZn_2Ge_2
$\text{Ba}_8\text{Zn}_7\text{Ge}_{39}$	10.756	43.024	$\text{Ba}_{7.95(3)}\text{Zn}_{7.1(1)}\text{Ge}_{38.9(1)}$	1% Ge
$\text{Ba}_8\text{Zn}_6\text{Ge}_{39}[\]_1$	10.747	42.988	$\text{Ba}_{8.00(2)}\text{Zn}_{6.3(1)}\text{Ge}_{39.7(1)}$	-
$\text{Ba}_8\text{Zn}_4\text{Ge}_{42}$	10.715	42.860	$\text{Ba}_{8.00(3)}\text{Zn}_{4.14(8)}\text{Ge}_{40.73(8)}$	2% $\text{Ba}_6(\text{Ge/Zn})_{25}$
$\text{Ba}_8\text{Zn}_3\text{Ge}_{40.5}[\]_{2.5}$	10.710	42.840	$\text{Ba}_{8.00(5)}\text{Zn}_{3.96(6)}\text{Ge}_{41.00(8)}$	10% $\text{Ba}_6(\text{Ge/Zn})_{25}$
$\text{Ba}_8\text{Zn}_2\text{Ge}_{41}[\]_3$	10.688	42.752	$\text{Ba}_{8.0(2)}\text{Zn}_{2.3(2)}\text{Ge}_{41.5(1)}$	44% $\text{Ba}_6(\text{Ge/Zn})_{25}$, 4% Ge

Table I. Nominal composition, lattice parameter of the type I clathrate, lattice parameter of the $a' = 4a$ superstructure, measured composition with EPMA of the clathrate and mass percentage of the secondary phases for the $\text{Ba}_8\text{Zn}_x\text{Ge}_{46-x-y}[\]_y$ samples. The EPMA measured compositions for $x \leq 6$ were obtained by normalizing at $[\text{Ba}] = 8$ while those for $x \geq 6$ were obtained by normalizing at $[\text{Zn}] + [\text{Ge}] = 46$ (see text for explanations).

Vacancies and site selectivity in $\text{Ba}_8\text{Zn}_x\text{Ge}_{46-x-y}$]_y

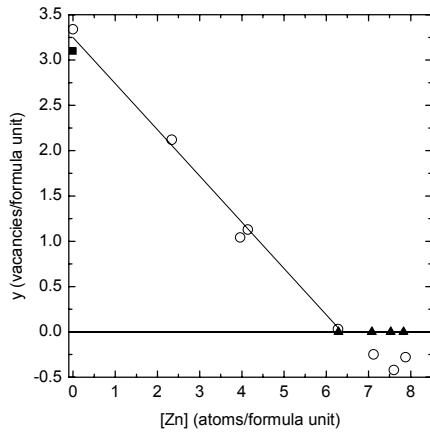


Figure 2. Number of vacancies (y) in $\text{Ba}_8\text{Zn}_x\text{Ge}_{46-x-y}$]_y as a function of the measured (EPMA) Zn fraction $[\text{Zn}]$. Open circles: $[\text{Ba}]$ normalized at 8. Filled triangle: $[\text{Zn}]+[\text{Ge}]$ normalized at 46. Filled square: $\text{Ba}_8\text{Ge}_{43}$]₃ vacancies number in reference [12]. The solid line is the best fit ($y = 3.3 - [\text{Zn}]/2$) to the experimental data for $0 \leq [\text{Zn}] \leq 6$.

A plot of the vacancies concentration (y), deduced from the relation $y = 46 - ([\text{Zn}] + [\text{Ge}])$, with $[\text{Zn}]$ and $[\text{Ge}]$ respectively the measured Zn and Ge elemental concentration, as a function of $[\text{Zn}]$ is displayed in Figure 2. It first shows that in the $\text{Ba}_8\text{Zn}_x\text{Ge}_{46-x-y}$]_y series, the vacancies concentration is fully dependent on the zinc concentration. y decreases linearly upon Zn substitution from ~ 3.3 for $[\text{Zn}] = 0$ to $y = 0$ for $[\text{Zn}] = 6$. A best fit of the data gives $y = 3.3 - [\text{Zn}]/2$ for $0 \leq [\text{Zn}] \leq 6$. The value $y = 3.3$ measured in $\text{Ba}_8\text{Ge}_{43}$]₃ by EPMA is consistent with the 3.1 Ge vacancies reported in $\text{Ba}_8\text{Ge}_{42.9}$]_{3.1} by energy dispersive spectroscopy [12]. These vacancies have also been shown to occur on the 6c site of the type I structure in $\text{Ba}_8\text{Ge}_{43}$]₃ [12]. If the zinc atoms exclusively substitute the Ge atoms and vacancies on the 6c site, one would expect that no vacancy remains when this site is completely filled by zinc atoms. In $\text{Ba}_8\text{Cd}_x\text{Ge}_{46-x}$]_y, Cd is reported to occupy very preferentially, but not exclusively, the 6c site when $x(\text{Cd}) < 6$ [13]. One also expects within this scenario that for zinc concentration larger than 6, the exceeding zinc atoms substitute on (an)other Ge site(s) and that the vacancies concentration remains equal to zero. However, in Fig. 2, for $[\text{Zn}] > 6$, an inconsistency appears since the vacancies concentrations are slightly negative (data represented by open circles). We think this effect indicates that vacancies (~ 0.05 / unit cell, see table I) occur on the barium sites for $[\text{Zn}] > 6$. The recent work on $\text{Ba}_8\text{Cd}_x\text{Ge}_{46-x}$]_y [13] also provided indications that such vacancies could occur on the Ba site. A change of normalization of the EPMA data from $[\text{Ba}] = 8$ to $([\text{Zn}] + [\text{Ge}]) = 46$ for $[\text{Zn}] > 6$ leads to the effective composition $\text{Ba}_{7.93}\text{Zn}_{7.53}\text{Ge}_{39.47}$ for $\text{Ba}_8\text{Zn}_8\text{Ge}_{38}$ sample B and shifts the circle to the $y = 0$ position of the triangle data points in Fig. 2. Based on their single crystal X-ray diffraction work, Kühl et al [7] had also concluded that

Zn fully substitutes the 6c site in $\text{Ba}_8\text{Zn}_x\text{Ge}_{46-x-y}$]_y. But their proposed relation $y = 4 - [\text{Zn}]/2$ between the vacancies concentration and the zinc concentration is not consistent with our data and with the fact that the vacancies occur on the 6c site.

Transport properties

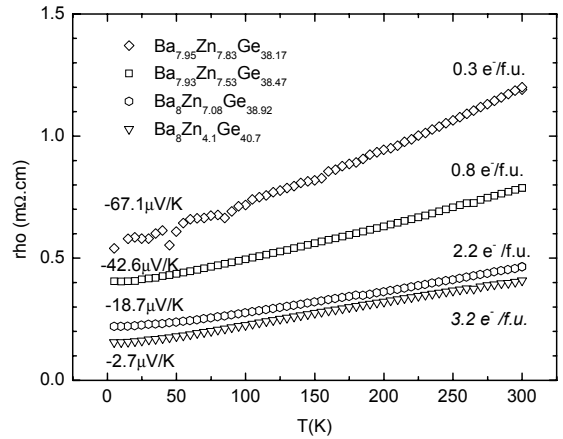


Figure 3. Thermal variation of the resistivity in $\text{Ba}_8\text{Zn}_x\text{Ge}_{46-x-y}$]_y. The room temperature value of the Seebeck coefficient and of the electron density ($[n]$) are also reported. $[n]$ is obtained from Hall effect measurements except in the $x = 4$ sample (italic) where it was calculated by the relation $[n] = 2([\text{Ba}] - [\text{Zn}]) - 4*y$ which assumes that vacancies behave like 4-electron acceptors.

The thermal variations of the resistivity in the $x = 4, 7, 8(\text{A})$ and $8(\text{B})$ samples are shown in Fig. 3. For all these samples, resistivity increases with temperature and its room temperature values range between 0.5 and 1.5 $\text{m}\Omega\cdot\text{cm}$. The weak variations of these resistivities with temperature are typical of “bad metals” or “degenerate semi-conductors”. This behaviour has previously been observed in $\text{Ba}_8\text{Ga}_x\text{Ge}_{46-x-y}$]_y polycrystals [8]. As expected, with increasing zinc concentration, the room temperature resistivity monotonously increases while the average electron density ($[n]$) derived from Hall effect measurements between 5-300K (not shown) consistently decreases. This is also consistent with the electron density which can be derived from the measured elements concentration, viz. $[n] = 2([\text{Ba}] - [\text{Zn}])$ for $[\text{Zn}] > 6$ ($y = 0$). Zinc effectively behaves like an 2-electron/atom acceptor and the $\text{Ba}_8\text{Zn}_x\text{Ge}_{46-x-y}$]_y fulfil the Zintl rules at least when $[\text{Zn}] > 6$. The absolute value of the room temperature Seebeck coefficient increases with $[\text{Zn}]$ and also strictly follows the electron density change. The sample with the largest power factor is $\text{Ba}_{7.95}\text{Zn}_{7.83}\text{Ge}_{38.17}$ with $\alpha^2/\rho = 3.75 \mu\text{W}\cdot\text{K}^{-2}\cdot\text{cm}^{-1}$ at 300K. It indeed shows that the compound with the largest measured zinc concentration (and closest to 8) and the lowest electron density of our series is the best one, similarly to the $\text{Ba}_8\text{Ga}_x\text{Ge}_{46-x-y}$]_y series [8]. Assuming a thermal conductivity similar to $\text{Ba}_8\text{Ga}_{16}\text{Ge}_{30}$, ($\lambda = 1.5 \text{ W}\cdot\text{m}^{-1}\cdot\text{K}^{-1}$), $ZT = 0.07$ at 300K in $\text{Ba}_8\text{Zn}_8\text{Ge}_{38}$. This value compares well

with $ZT = 0.09$ at 300K published for polycrystalline $Ba_8Ga_{16}Ge_{30}$ by Kuznetsov et al. [14]. More transport measurements at high temperature are required to determine the potential for thermoelectric power generation of $Ba_8Zn_8Ge_{46}$.

Conclusions

Our X-ray powder measurements indicate that the $Ba_8Zn_xGe_{46-x}$ ($4 < x < 8$) compounds crystallize within a $4ax4ax4a$ superstructure of the type I clathrate structure. EPMA shows that the vacancies concentration varies like $y = 3.3 - [Zn]/2$ for $[Zn] < 6$ and that $y = 0$ for $[Zn] > 6$. It also confirms that Zn substitutes on the 6c site of the approximant type I structure. Resistivity versus temperature (5K-300K) data ($x > 6$) are in line with a degenerate semi-conducting behaviour and evolves consistently with x and the electron density. $Ba_8Zn_8Ge_{30}$ shows the largest power factor in our series ($\alpha^2/\rho = 3.75 \mu W \cdot K^{-2} \cdot cm^{-1}$) and a ZT value at 300K slightly smaller than $Ba_8Ga_{16}Ge_{30}$.

References

- 1 Nolas, G. S. *et al.*, Semiconducting Ge clathrates: promising for thermoelectric applications, *Applied Physics Letters*, Vol. 73 (1998), pp. 178.
- 2 Saramat, A. *et al.*, Large thermoelectric figure of merit at high temperature in Czochralski-grown clathrate $Ba_8Ga_{16}Ge_{30}$, *Journal of Applied Physics*, Vol. 99 (2006), pp. 023708.
- 3 Anno, H. *et al.*, Thermoelectric properties of $Ba_8Ga_xGe_{46-x}$ clathrate compounds, *Proc 21st International Conference on Thermoelectrics- Long Beach, California, USA - Aug. 25-29, 2002*, pp. 77.
- 4 Bontien, A. *et al.*, High temperature thermoelectric properties of alpha and beta- $Eu_8Ga_{16}Ge_{30}$, *Proc 22nd International Conference on Thermoelectrics ICT2003, La Grand Motte, France, August, 2003*, pp. 131.
- 5 Blake, N. P. *et al.*, Structure and stability of the clathrates $Ba_8Ga_{16}Ge_{30}$, $Sr_8Ga_{16}Ge_{30}$, $Ba_8Ga_{16}Si_{30}$, and $Ba_8In_{16}Sn_{30}$, *Journal of Chemical Physics*, Vol. 114, No. 22 (2001), pp. 10063.
- 6 Madsen, G. K. H. *et al.*, Electronic structure and transport in type-I and type-VIII clathrates containing strontium, barium, and europium, *Physical Review B*, Vol. 68 (2003), pp. 125212.
- 7 Kuhl, B. *et al.*, Neue ternäre Käfigverbindungen aus den Systemen Barium-Indium/Zinc/Cadmium-Germanium: Zintl-Verbindungen mit Phasenbreite ?, *Zeitschrift fuer Anorganische und Allgemeine Chemie*, Vol. 621 (1995), pp. 1.
- 8 Okamoto, N. L. *et al.*, Crystal structure and thermoelectric properties of type-I clathrate compounds in the Ba-Ga-Ge system, *Journal of Applied Physics*, Vol. 100 (2006), pp. 073504.
- 9 Rodriguez-Carvajal, J., FULLPROF, *Physica B*, Vol. 192 (1993), pp. 55.
- 10 LeBail, A. *et al.*, Ab Initio structure determination of $LiSbWO_6$ by X-ray powder diffraction, *Materials Research Bulletin*, Vol. 23 (1988), pp. 447.
- 11 Bérardan, D. *et al.*, Preparation and chemical properties of the skutterudites $(Ce-Yb)_yFe_{4-x}(Co/Ni)_xSb_{12}$, *Materials Research Bulletin*, Vol. 40, No. 3 (2005), pp. 537.
- 12 Carrillo-Cabrera, W. *et al.*, Ba_8Ge_{43} revisited: a $2a'x2a'x2a'$ Superstructure of the Clathrate-I Type with Full Vacancy Ordering, *Zeitschrift fuer Anorganische und Allgemeine Chemie*, Vol. 630 (2004), pp. 2267.
- 13 Melnychenko-Koblyuk, N. *et al.*, Ternary clathrates Ba-Cd-Ge: phase equilibria, crystal chemistry and physical properties, *Journal of Physics : Condensed Matter*, Vol. 19 (2007), pp. 046203.
- 14 Kuznetsov, V. L. *et al.*, Preparation and thermoelectric properties of $A(8)(II)B(16)(III)B(30)(IV)$ clathrate compounds, *Journal of Applied Physics*, Vol. 87, No. 11 (2000), pp. 7871.